

# ANN Control Based on Patterns Recognition for A Robotic Hand Under Different Load Conditions

Ihsan Abdulhussein Baqer Mauwafak Ali Tawfik Hayder Ahmed Abdulrazzaq

*Mechanical Engineering Department , University of Technology*

[ihsan.qadi@gmail.com](mailto:ihsan.qadi@gmail.com)

[drmat19853@yahoo.com](mailto:drmat19853@yahoo.com)

[haider93.hh94@gmail.com](mailto:haider93.hh94@gmail.com)

## Abstract

In this paper, the Artificial Neural Network (ANN) is trained on the patterns of the normal component to tangential component ratios at the time of slippage occurrence, so that it can be able to distinguish the slippage occurrence under different type of load (quasi-static and dynamic loads), and then generates a feedback signal used as an input signal to run the actuator. This process is executed without the need for any information about the characteristics of the grasped object, such as weight, surface texture, shape, coefficient of the friction and the type of the load exerted on the grasped object. For fulfillment this approach, a new fingertip design has been proposed in order to detect the slippage in multi-direction between the grasped object and the artificial fingertips. This design is composed of two under-actuated fingers with an actuation system which includes flexible parts (compressive springs). These springs operate as a compensator for the grasping force at the time of slippage occurrence in spite of the actuator is in stopped situation. The contact force component ratios can be calculated via a conventional sensor (Flexiforce sensor) after processed the force data using Matlab/Simulink program through a specific mathematical model which is derived according to the mechanism of the artificial finger.

**Key words:** Slippage detection, Neural network algorithm, Artificial hand, Normal and Tangential force, Tactile sensors.

## الخلاصة

في هذا البحث، الشبكة العصبية الاصطناعية (ANN) قد تم تدريبها على انماط نسب المركبات العمودية الى الافقية لقوى التماس عند وقت حدوث الانزلاق، لتكون قادرة على تمييز الانزلاق تحت انواع مختلفة من الأحمال (الحمل الستاتيكي والحمل الديناميكي)، ومن ثم توليد اشارة راجعة تستخدم كمشغل لمحرك اليد الصناعية. هذه العملية اجريت بدون الحاجة لأي معلومات حول خواص الجسم الممسوك، مثل الوزن، تركيب السطح، الشكل، معامل الاحتكاك و نوع الحمل المؤثر على الجسم الممسوك. لتحقيق ذلك، تم اقتراح تصميم جديد لرأس الاصبع من اجل كشف الانزلاق في اتجاهات متعددة بين الجسم الممسوك ورؤس الاصابع الاصطناعية. هذا التصميم يتألف من اصبعين مع نظام تشغيل يتضمن اجزاء مرنة (نوابض انضغاطية). هذه النوابض تعمل كمعوض لقوة المسك عند وقت حدوث الانزلاق حتى في وضعية التوقف لمحرك اليد. نسب مركبات قوى التماس يمكن حسابها بواسطة حساسات قوى تقليدية (FlexiForce sensor) بعد معالجة بيانات القوى باستخدام برنامج Matlab/Simulink ومن خلال علاقات رياضية معينة التي تم اشتقاقها لوصف الآلية الميكانيكية للإصبع الاصطناعي.

**الكلمات المفتاحية:** كشف الأنزلاق، خوارزمية الشبكة العصبية، اليد الاصطناعية، القوة العمودية والماسية، اجهزة الاستشعار عن طريق اللمس.

## 1. Introduction

The interest of tactile sensing has been increased in the field of robotics. It allows for the robots to interact with an environment physically and adjust it by improving the essential capabilities. These capabilities are represented by touching, collisions and detecting slippage. Advanced capabilities are represented by manipulation of object and

grasping (Fernandez *et.al.*, 2014). One of these characteristics that must be improved is the detection of the slip. The slippage recognition between two surfaces regards necessary sensing should operate at the slippage time occurrence. To fulfil of the slippage sensing operation, it is needed to use a multi-sensory system to acquire an indication of the first stage of slip. On the other hand, the incipient slippage should be prevented by interpreting the signal of a multi-sensory system (the signal of slip) and send it to the actuator as a feedback signal to increase the magnitude of the grasping force. The artificial intelligent algorithm plays an essential role in this operation through obtaining a slipping signal that is considered as input information and generating the feedback signal (Somer *et.al.*, 2016).

In the field of the slippage control via artificial intelligence, there are many of the studies. Some of the previous studies, (Fusjimoto *et.al.*, 2003) proposed a method to realize the sensation of static friction using an artificial finger skin piece for robotic hand, where this hand contains two embedded strips of PVDF film to detect slip via ANN. (Ikeda *et.al.*, 2004) presented a method of controlling gripping forces of an elastic-object based on the feedback of a visual slip margin; however, to embrace that a one degree of freedom gripper composed of a force sensor and camera was used. The grip forces were controlled via a direct feedback of margin to provide the desired value of gripping force. (Chen *et.al.*, 2006) introduced a method for grasping control of artificial hand by means of partially linearized ANN and possibility theory to detect the slip onset between the artificial hand and the held object. The artificial hand contains Double-Octagon tactile sensor which is used to measure the grasping forces. (Mazid and Fakhrul, 2008) introduced mathematical relationships for computing the vibration scattered energy. These vibrations were sensed via the stylus at the period of slippage occurrence. The ANN is employed to provide an optimal force for grasping the object depending on its Physio-mechanical characteristics. (Herrera, 2011) suggested a model of tactile control for lifting the objects which were not defined in controller, where this process being in a stable status of grasp and similar to the behavior of the human grasp. The process has been done with the aid of ANN algorithm which was used to determine the coefficient of friction and to detect the initial slip. (Robert *et.al.*, 2012) presented a method to recognize incipient slippage in high-speed, by utilizing the resistive sensing principle, which represented by piezo-resistive tactile sensor. It was noticed through tests that each surface texture generates different frequency spectra. To estimate the velocity of slippage in different object with different texture an ANN is trained to classify the frequency spectra. (Joonhee *et.al.*, 2012) presented an attempt to control a grasping force by controlling the robot's hand velocity using Force/Torque sensor (FTS) which produces a command torque, which then converted via the velocity-torque transformer into the input velocity of the system of the artificial hand for providing a stable holding with the desired forces of grasping. (ShouheiShirafuji and KohHosoda, 2014) displayed a description of a specific technique by which the robotic hand can be controlled by depending on the previous experience of the grasped object's slippage. To achieve this, it has been used two sensors. The first sensor is PVDF films which are used to detect the changes of the pressure i.e. they used for detecting slippage. The second sensor is strain gauges which are used to determine the stresses. The determined stresses were utilized as input data for ANN which controls the robotic actuation system. (Kobayashi *et.al.*, 2014) used force/torque sensor, which measures pressure distribution to detect slip. Rather than increasing

gripping force, it was proposed more fingers to be applied in order to stop slipping. (Abdulrahman *et.al.*, 2016) developed intelligent of robotic hand, including optimum force of gripping and analysis of slippage. Two FSR sensors had been used to measure the continuous force of gripping between the object and the robotic hand. In addition, the rotary encoder device was used to apply the automatic feedback response. The feedback response was applied to prevent the slip continuity status.

As a summary, a lot of researchers studied the problem of controlling the slippage which is produced by acting of the external loads that presented as quasi-static or static load exerted upon the grasped object and in one direction of slippage occurrence. This is due to the utilized sensors or the techniques of the slip detection. These sensors unable to distinguish between the variance in the signal that caused by the effect of the external disturbances upon the grasped object or that caused by the effect of slipping. In the present work, The proposed design deals with the conventional sensors that have the ability to measure only the applied forces in the normal direction, but in this work, they employed to measure the three components of the contact forces by processed the signals through a mathematical model. Also, the advantage of the proposed system is detecting the slip without knowing any characteristic of the grasped object such as weight, coefficient of friction, shape, surface texture and the excitation type that exerted upon the grasped object.

## 2. Mathematical Model

Figure (1) shows a fingertip mechanism of artificial hand, which is designed as a dome-shape that represents the area of contact with the grasped object. Also, it is connected with the finger links by ball joint. The figure (2) represents the installation of the flxiforce sensors and the compressive springs within the robotic fingertip structure.

The fingertips were covered with a soft material, which have a ridged surface, in order to overcome the problems that arise in rigid fingertips, which include: (1) the impact force which is generated at the instant of grasping the rigid object. Tact force may affect the fingertip sensors functioning. (2) The artificial hand with rigid fingertips cannot provide securely grasp object which contains uneven surfaces because of the poor conformability of the artificial fingertips. (3) The repetitive strains which are generated in the fingertips throughout the manipulation tasks (Elango and Faudzi, 2015).

The mathematical model of the artificial fingertips has been derived to create the relationship between the components of the contact force and the forces exerted on the force sensors.

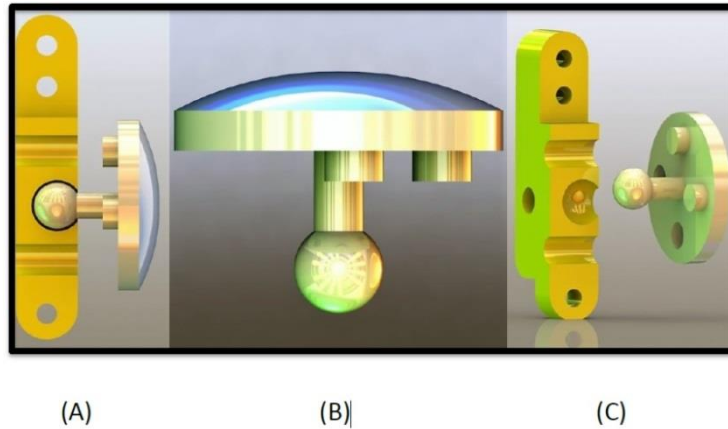


**Figure (1): The proposed Mechanism of the artificial fingertip.**

- (A) Side view of fingertip part and its frame
- (B) Side view of Fingertip part
- (C) 3D view, fingertip part release from its frame

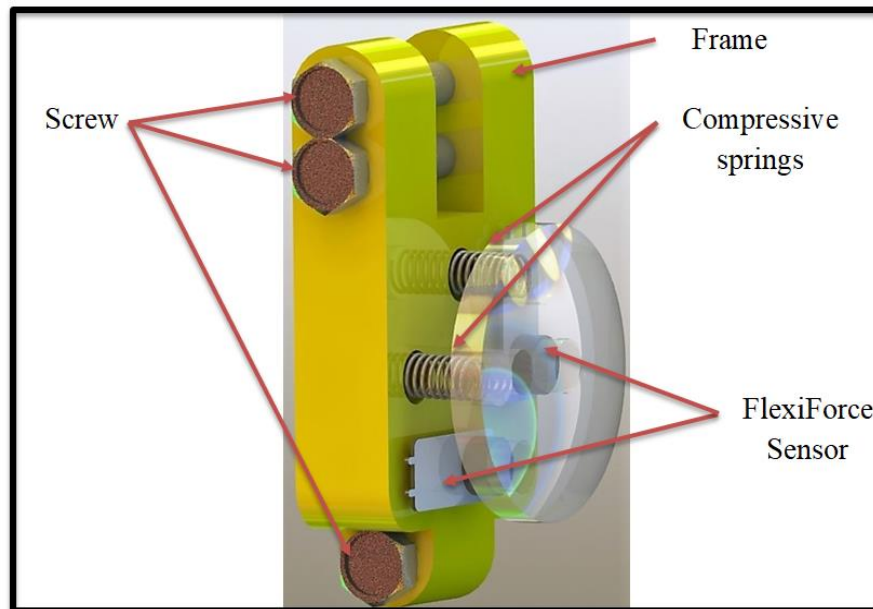


**Figure (2): FlexiForce Sensors and springs setup with the Fingertip.**

For simplicity, it is assumed that there is no relative motion between the fingertip and the grasped object before slip occurrence; also, the ball joint friction and the inertia of the fingertip are neglected (Mark, 1989). Figure (3) represents the distribution of the contact force components, forces exerted on the sensors and springs forces, where these forces can be analyzed statically to find both normal and tangential force component w.r.t force sensors.

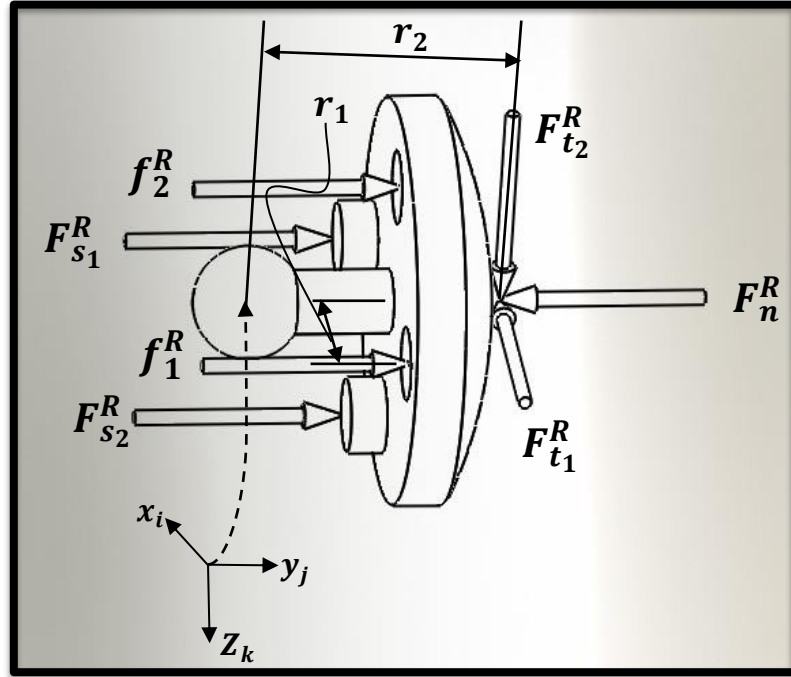


**Figure (3): Fingertip Free Body Diagram.**

By summation of the forces in y-axis it can be found the normal force  $F_n^R$ :

$$+\uparrow \sum F_y = 0$$

$$F_n^R = F_{s_1}^R + F_{s_2}^R + f_1^R + f_2^R \quad (1)$$

From the moment equilibrium equations of the fingertip for three axes in a vector notation about its ball joint the two tangential force components can be determined as follows:

$$(r_2 j \times F_{t_2}^R k) + (r_2 j \times F_{t_1}^R i) + ((-r_1) i \times f_1^R j) + ((-r_1) k \times f_2^R j) + (r_1 i \times F_{s_1}^R j) + (r_1 k \times F_{s_2}^R j) = 0 \quad (2)$$

For  $i = i$  &  $k = k$ , and after mathematical simplification, gives:

$$F_{t_1}^R = \frac{F_{s_1}^R * r_1 - f_1^R * r_1}{r_2} \quad (3)$$

And,

$$F_{t_2}^R = \frac{F_{s_2}^R * r_1 - f_2^R * r_1}{r_2} \quad (4)$$

By the same way, the normal and tangential force components of the left finger will be obtained as:

$$F_n^L = F_{s_1}^L + F_{s_2}^L + f_1^L + f_2^L \quad (5)$$

$$F_{t_1}^L = \frac{F_{s_1}^L * r_1 - f_1^L * r_1}{r_2} \quad (6)$$

And,

$$F_{t_2}^L = \frac{F_{s_2}^L * r_1 - f_2^L * r_1}{r_2} \quad (7)$$

Now, dividing the two tangential forces of each finger on their normal forces in order to obtain the ratios of contact force components in X-Y plane and Z-Y plane as follows:

In X-Y plane:

$$\frac{F_{t_1}^R}{F_n^R} = \frac{F_{s_1}^R * r_1 - f_1^R * r_1}{(F_{s_1}^R + F_{s_2}^R + f_1^R + f_2^R) * r_2}, \quad \frac{F_{t_1}^L}{F_n^L} = \frac{F_{s_1}^L * r_1 - f_1^L * r_1}{(F_{s_1}^L + F_{s_2}^L + f_1^L + f_2^L) * r_2} \quad (8)$$

And in Z-Y plane:

$$\frac{F_{t_2}^R}{F_n^R} = \frac{F_{s_2}^R * r_1 - f_2^R * r_1}{(F_{s_1}^R + F_{s_2}^R + f_1^R + f_2^R) * r_2}, \quad \frac{F_{t_2}^L}{F_n^L} = \frac{F_{s_2}^L * r_1 - f_2^L * r_1}{(F_{s_1}^L + F_{s_2}^L + f_1^L + f_2^L) * r_2} \quad (9)$$

From the stability of the grasp status and the friction cone definition, the contact force component ratio must be within the friction cone,

$$\frac{F_{t_i}}{F_{n_i}} \leq \mu_i \quad (10)$$

But, the texture of the grasped object surface and the coefficient of friction are unknown. In this case, the slippage cannot be distinguished by using equation (10). So, the slip detection should be done through monitoring the variation in the result of an equation (9) with real time.

### 3. System Description

#### 3.1 Robotic gripper

An artificial two-finger gripper is set up at the end of four degrees of freedom artificial robotic arm. The robotic gripper is under-actuated, as shown in the figure (4), where it consists of DC geared motor which is connected to power screw in order to convert the motion from rotational at the DC motor to linear at constrained nut. The nut is connected with three springs that transmit the linear motion to cylindrical part which

associated with the links which form the finger structure. Connection the springs between the nut and the cylindrical part allows the artificial hand to adapt the grasping force in spite of the actuator is in a stationary status.

### 3.2 Sensors

A FlexiForce sensor model A301 (<https://www.tekscan.com/products-solutions/force-sensors/a301>) has been used in this work. It is mounted within the fingertip as shown in figure (2). It can measure the applied force on its sensing area in one direction, but in this work it is used to measure all the contact force components with 445 N range of force. Also, a hall-effect sensor 49E model (<https://chioszrobots.com/2015/03/26/hall-magnetic-standard-linear-module-arduino-projects-robots-new/>) has been used to give an indication of the slippage situation by observing the variation in relative motion between the palm of the gripper and the grasped object, as clarified in figure (4). The signal of the hall-effect device was not calibrated because it is used only for slip monitoring. All the mentioned sensors generate an analog signal that is transformed to digital signal from a data acquisition device (National Instruments USB-6009), and then the digital signal is transmitted to a PC in order to process it by Matlab-Simulink program.

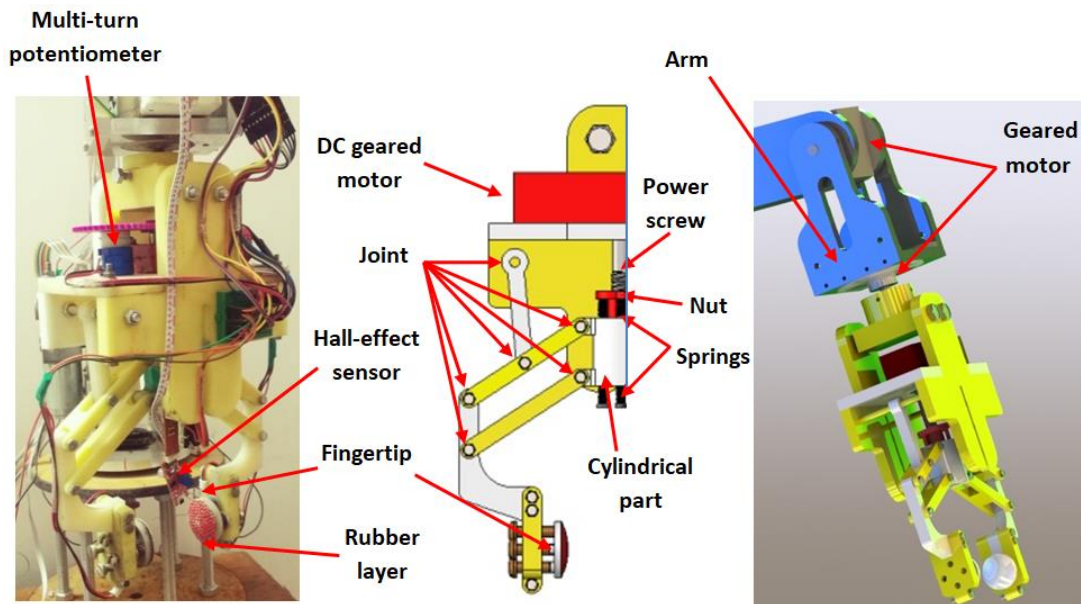


Figure (4): Robotic gripper mechanism.

### 3.3 Grasped Object

The grasped object is designed in a cuboid shape with two disturbance generators (unbalance DC motors) embedded within the grasped object as clarified in Figure (5)) to generate an excitation that is used as an external dynamic load. Each two corresponding layer at the contact zone of the grasped object with the fingertip is covered by one type of the typical material, namely, glass and wood layers as the test requires as shown in figures (5).

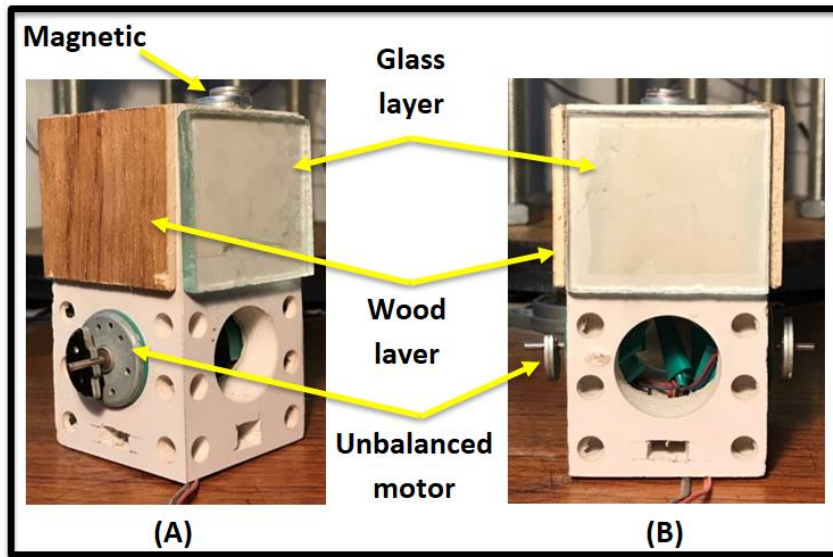


Figure (5): (A) 3D view and (B) side view of experimental

#### 4. Control System structure

This section introduces the control system which is represented by the Artificial Neural Network. During the period in which the slippage occurs, all the variables that mentioned in section (2) must be monitored in order to recognize the moment of the slippage occurrence. Therefore, an artificial intelligence algorithm has been configured to state the onset of slippage. This algorithm has been made by using the pattern recognition in Neural Network - Matlab. This software is based on a feedforward and backpropagation neural network algorithm, which composed of an input layer, two hidden layers each has ten neurons and output layer with two neurons, as depicted in figures (6) and (7).

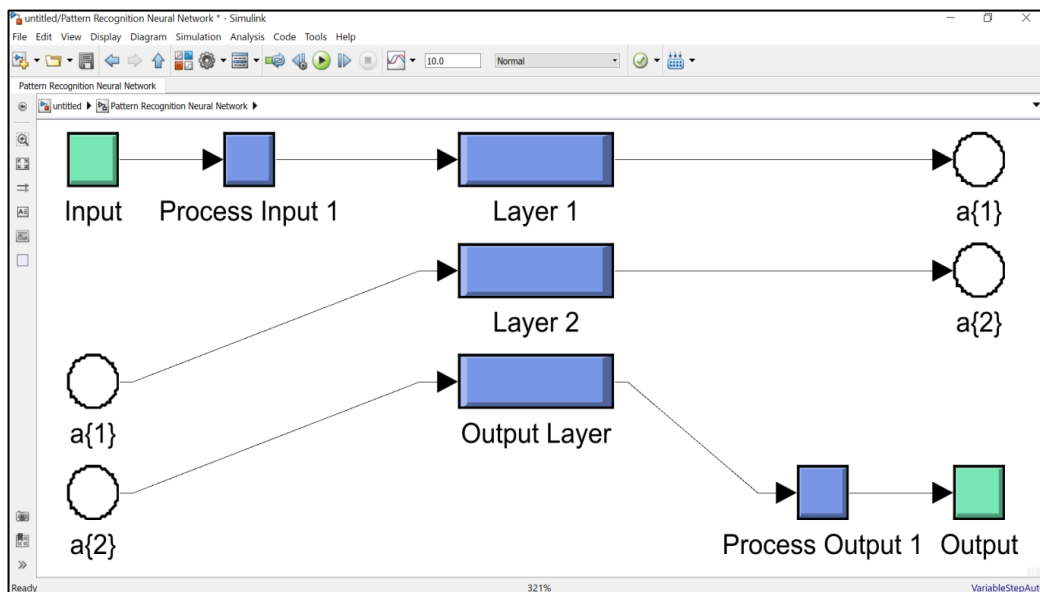


Figure (6): Neural Network Simulink diagram.

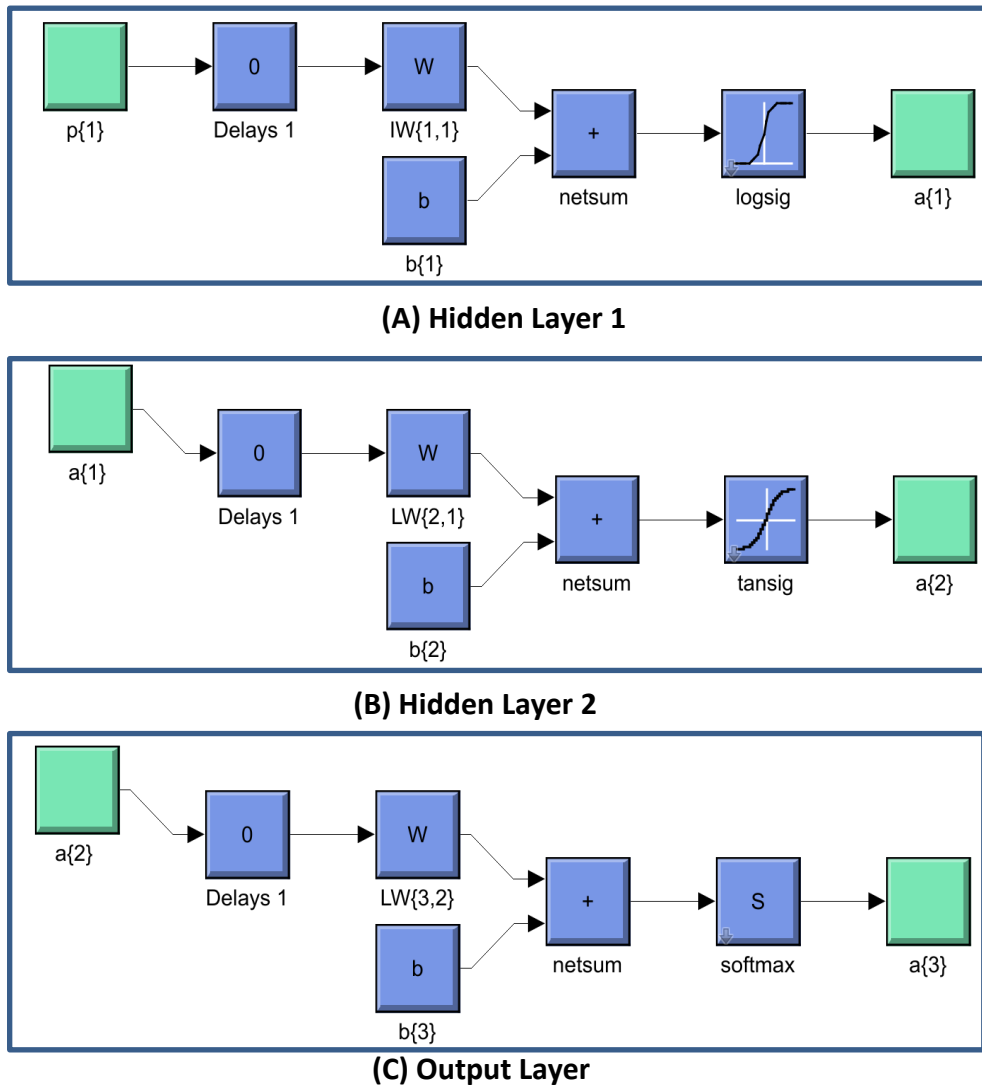


Figure (7): Structure of Neural Network Layers.

## 5. Results and Discussion

### 5.1 Data set for Artificial Neural Network Training

There are three groups of experiments to force the grasped object to slip. After that, the slippage data are acquired by the sensory system. The objective of these experiments is to demonstrate the effectiveness of the proposed system to detect slipping in multi-direction under different types of loads. The experiments will be explained as follows:

**5.1.1 First Experiments Group:** grasping the object under the effect of external pulling (quasi-static load).

This group of experiments is performed as in the following sequence:

- (1) Grasping the object by means of turning-on the robotic gripper actuator until it reaches the stable status of grasp.
- (2) Start recording the signals of the sensory system at the moment when the grasping reaches the stable status.
- (3) Pulling the grasped object manually until it starts to slip;
- (4) Restarting the previous steps, but in a different slippage direction.

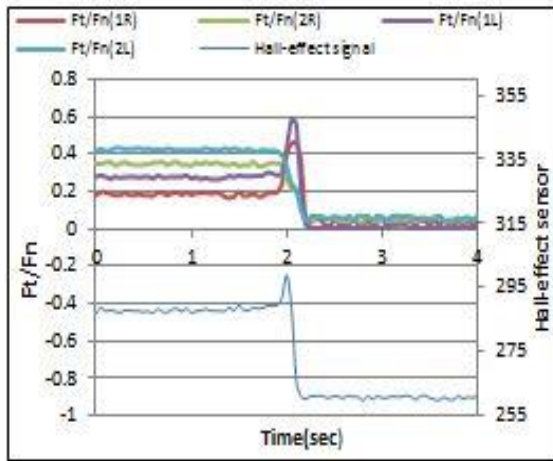


**Figure (8):** The forces ratio versus time with angle slipping of 0 deg.

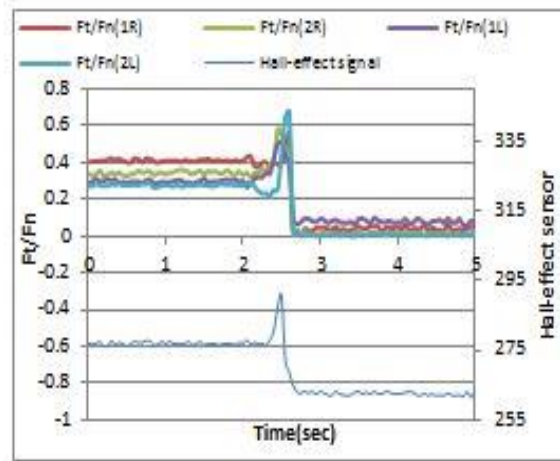


**Figure (9):** The forces ratio versus time with angle slipping of 45 deg.

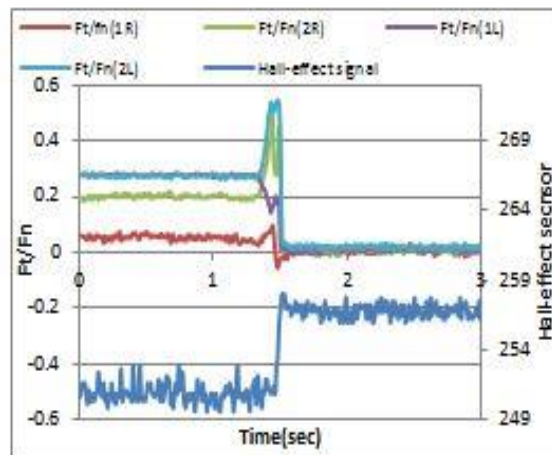


**Figure (10):** The forces ratio versus with angle slipping of 90 deg.

From the results of the first experiment group, one can observe that the signal behavior of the contact force component ratio in real time starts with a certain ratio of initial grasping force. This force ratio varies from one to another experiment due to the effect of the compressive springs in the fingertip structure, and then this signal will vary as a jump from the initial value at the moment of slip occurrence. Also at this time, the variation in the Hall-effect sensor signal will be occurred approximately similar to the variation in the signal of force ratio, this means the beginning of the grasped object slippage. Furthermore, it was observed that the variation in the signal of ratios ( $F_{t_i}/F_{n_i}$ ) changes according to the angle of slippage occurrence. When the slippage angle is 0 deg, the variation in the signal just occurs in the force ratios that oriented towards z-axis, when the slippage angle is 40 deg, the jump in the signal occurs at the force ratios in both x-axis and z-axis in a similar behavior, and when the slippage angle is 90deg, the variation in signal just occurs in the force ratios that oriented towards the x-axis.

**5.1.2 Second Experiments Group:** grasping the object under the effect of external disturbance (dynamic load).

These experiments are performed as in the previous sequence as mentioned in the first group of experiments except step. 3; However, in these experiments the unbalance motors have been used as disturbance generators in order to generate slippage between the grasped object and the fingertip at the moment of its turning-on. The results of this group will be listed and presented in figures (11) to (13):

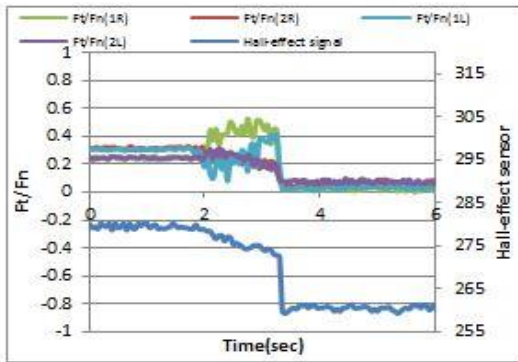


**Figure (11):** The forces ratio versus with angle slipping 0 of deg.

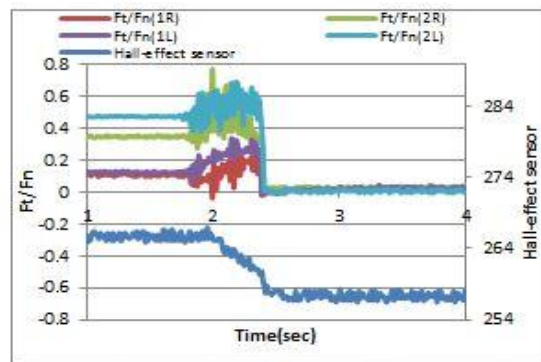


**Figure (12):** The forces ratio versus time with angle slipping of 45 deg.

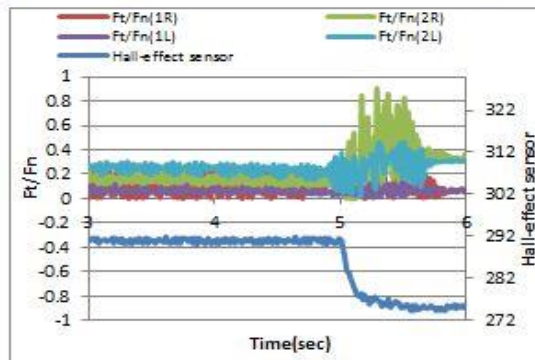


**Figure (13):** The force ratio versus time with angle slipping of 90 deg.

In these experiments, as the dynamic load is applied, the object begins to slip, also at this moment; the signal of force ratio is starting to change into a form of an alternative sequence, this change is due to the instantaneous variation that occurs in the magnitude and direction of the components of the contact forces. Subsequently, the friction cone condition cannot be satisfied because of the variation range of force ratio will be raised during the period of slippage occurrence in comparison with the drop in friction coefficient from static ( $\mu_s$ ) to dynamic ( $\mu_d$ ). Also, it was observed that the response of the contact force component ratios varies depending on the angle of slip, namely, only the ratio that is towards the angle of slip will get the variation in its signal as explained in the first group of experiments.

The training of the artificial neural network has been done by means of importing a data from the experimental results of equations (7) and (8), in other words, the signals of the components of the contact forces under quasi-static and dynamic loads. These data are randomly shuffled to increase the depth of learning for this algorithm so that it can recognize the occurrence of the slippage at any time. The collected data are divided into specific time interval. Afterwards, these data are converted into a vector form by passing through a buffer block in Matlab-Simulink program. This block makes the signal is divided to be an input vector of artificial neural network. The following figure shows the schematic diagram of the buffering process:

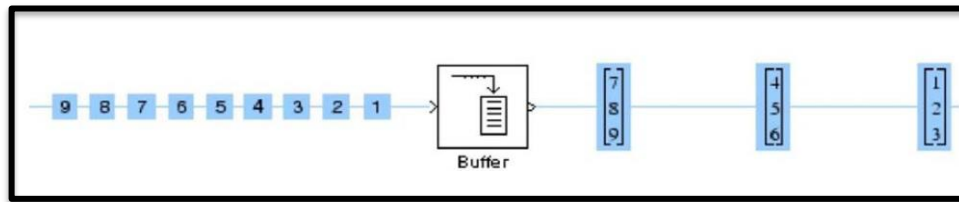


**Figure (14): the buffering process schematic diagram**

After buffering the ratio signals ( $F_{t_i}/F_{n_i}$ ), the output vector (target vector) of the trained algorithm is in the form of a binary system (0 , 1) based on recognizing the signal behavior of the ratios of contact force components, when the target vector value is  $[0 \ 1]^T$ , this means that there is no slippage. While when the target vector value is  $[1 \ 0]^T$ , this means that there is a slippage. In the case of the slippage occurrence, the signal of force ratios will jump. The training has been done in different grasping force levels and for two different materials (glass and wood). Figures (15) and (16) display the ability of the artificial neural network to recognize the behavior of the contact forces ratios signal at the duration of the slip under different loads (quasi-static and dynamic) with (10) hidden layer neurons and (10) input layer size.

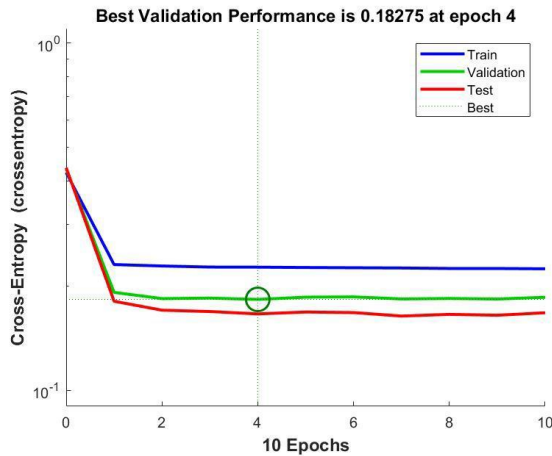


**Figure (15):** The performance of ANN with (10) input layer size, (10) hidden layer neurons and two hidden layers, under quasi-static load.

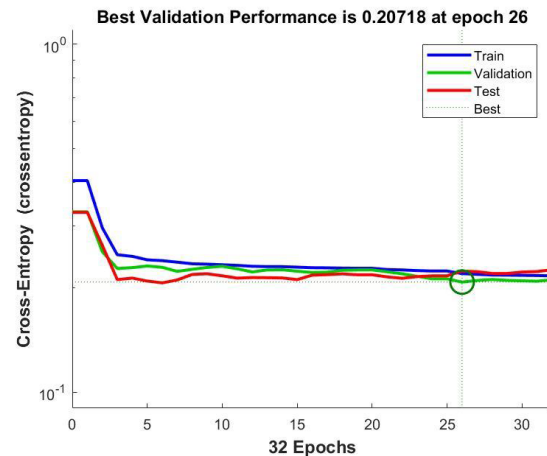


**Figure (16):** The performance of ANN with (10) input layer size, (10) hidden layer neurons and two hidden layers, under dynamic load.

## 5.2 Enhancement of Performance of Artificial Neural Network by Using Input Normalization

As clarified in figures (15) and (16), the neural network was responding with a poor ability of training; therefore, the signals of contact force component ratio are normalized. The normalization process is done through subtracting the signals of force ratio from their instantaneous mean values for minimizing the diversity from one sample to another. To fulfil this process, a special model by using Matlab-Simulink program was built as clarified in figure (17).

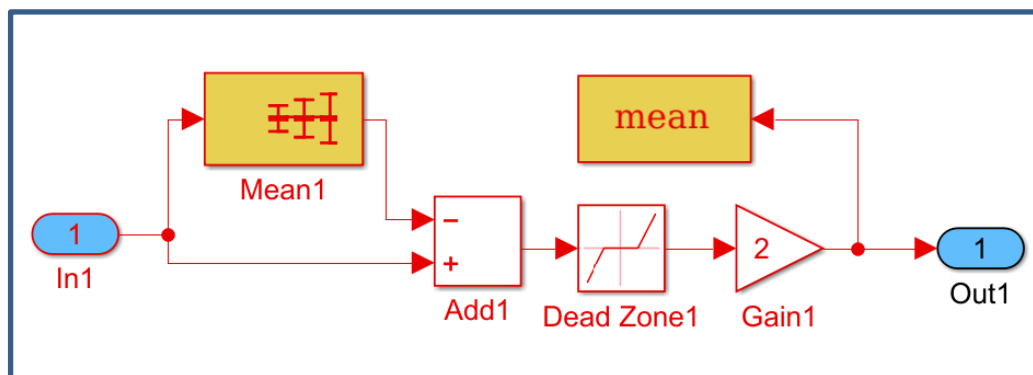


**Figure (17):** The Normalization process block diagram.

This aids the neural network algorithm to reach the best performance, as displayed in figures (18) and (19).

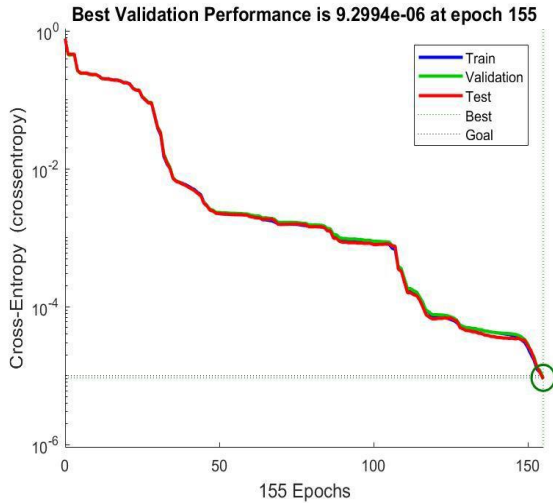


**Figure (18):** The performance of ANN after Normalization with (10) input layer size, (10) hidden layer neurons and two hidden layer, under quasi-static load.

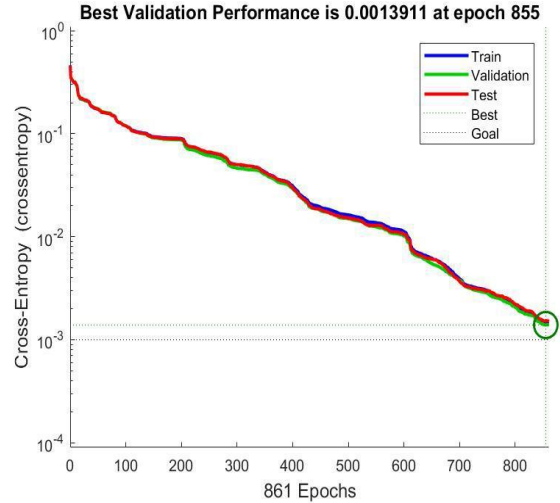


**Figure (19):** The performance of ANN after Normalization with (10) input layer size, (10) hidden layer neurons and two hidden layer, under dynamic load.

From the previous figures (18 & 19), one can notice, at the quasi-static case, the Artificial Neural Network cross entropy became (9.2994e-06) at best validation performed and 155 epoch as shown in figure (18), while at the dynamic case, the cross entropy became (0.001394) at best validation performed and 855 epoch as shown in figure (19).

### 5.3 ANN Experiments for detecting and controlling slippage

The experiments are done for different contact material of the grasped object (glass and wood) and for different grasping force levels. When the neural network trains under different conditions of grasping, the control system appears a high ability to distinguish the behavior of the signal at the slippage occurrence period. The output of the control system will be in the form of two vectors; [1 0] this denotes the stable grasping situation, while [0 1] denotes slippage situation and sending an order to turning-on the hand's actuator. The tests to control the slippage will be divided into two groups and summarized as follows:

**5.3.1 First group of experiments:** Control the slippage under quasi-static load cases.

To evaluate the Artificial Neural Network performance for detecting slippage, the controlling system is examined experimentally by monitoring the moment of system response when a variation in the normalized signal of force ratio occurs under quasi-static load cases. The process of these experiments has been begun by grasping the object just under the object weight effect (stable grasping conditions). Afterwards, the grasped object was pulled manually to force it to slip.

These experiments have been conducted in different angles of slippage for three times, and then repeating these experiments again, but with a pair of contact material of the grasped object (wood, glass). The results of these experiments will be listed as subfigures within figures (20) (20) (22) and (23):

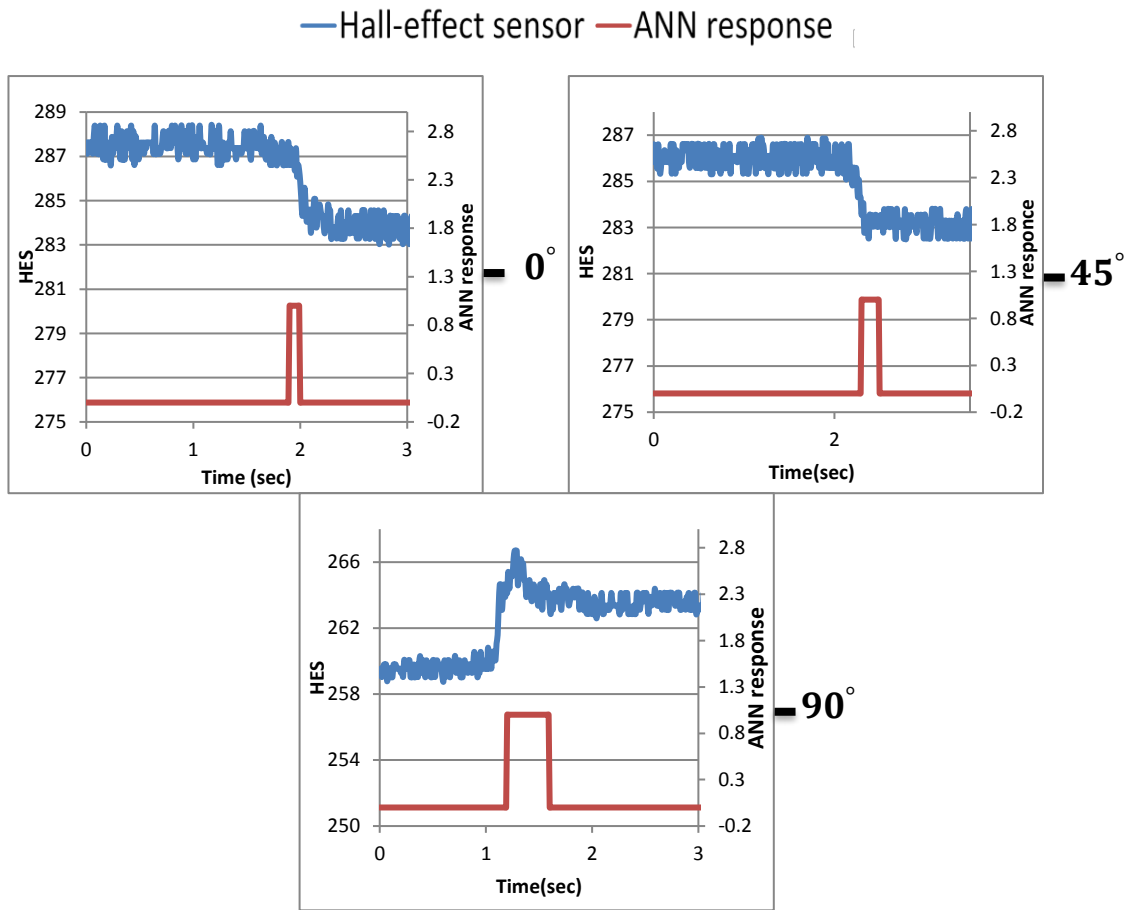


**Figure (20): The system control response under quasi-static load and different slippage angles, glass layer.**

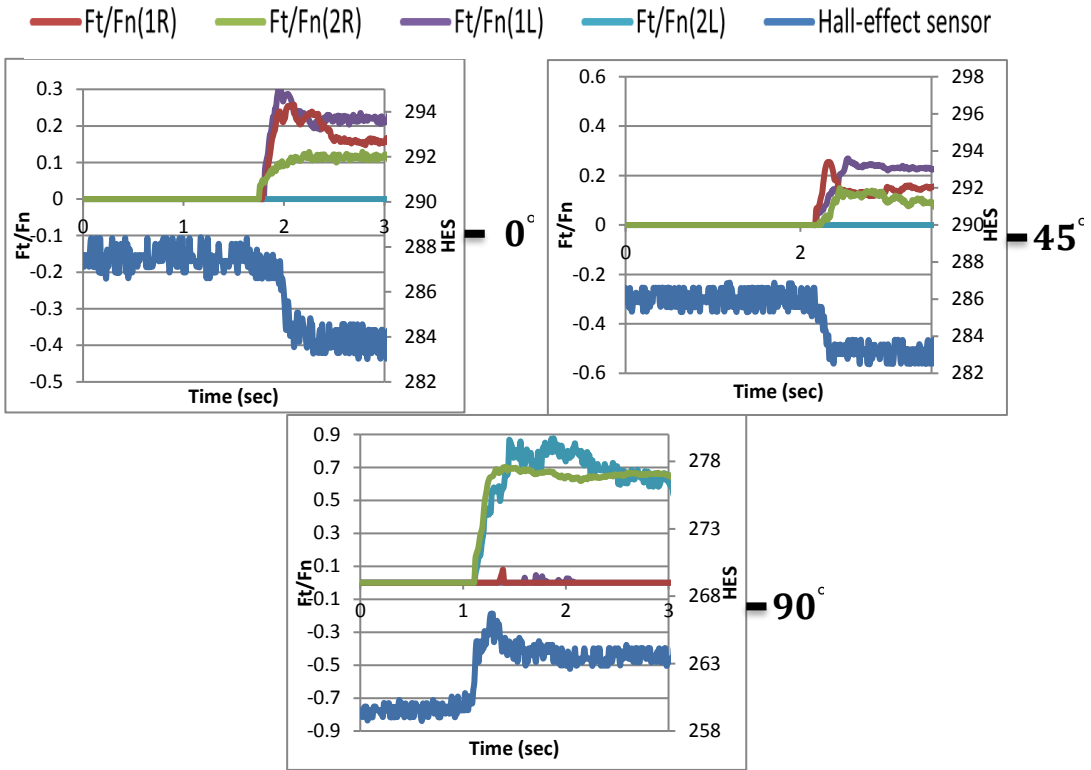


Figure (21): The normalized force ratios under quasi-static load and different slippage angles, glass layer.

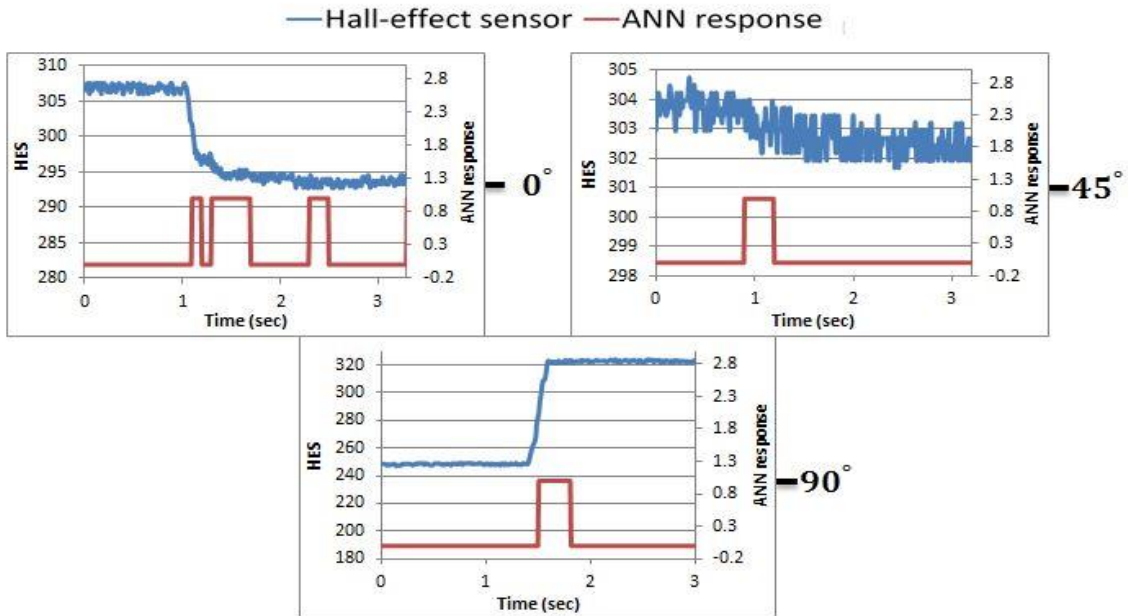
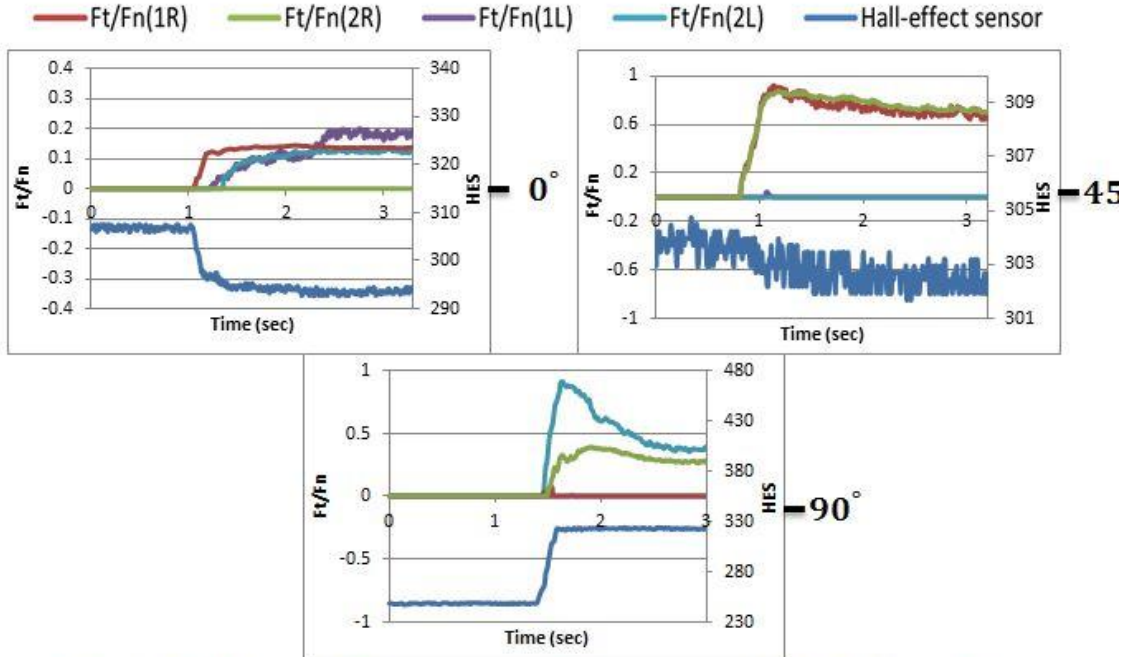


Figure (22): The system control response under quasi-static load and different slippage angles, wood layer.



**Figure (23): The normalized force ratios under quasi-static load and different slippage angles, wood layer.**

Each experiments graph in figure (20) and (22) clarify the feedback response of artificial neural network with time for different slippage angles and different contact materials in comparison with the signal of the hall-effect sensor (HES). One can observe any variation in the magnitude of its signal when there is any relative motion between the grasped object and the fingertips (slippage occurrence). From these experiments, it can be noticed, that the artificial neural network gives an excellent response with different slippage angles. This means that the controller does not need to know the slippage at any angle happened in order to detect and control it. Also, it was observed, when the contacting occurs between the soft layers of the fingertips and the pair of glass layers of the grasped object, the grasping process is more stable and the results of experiments of this case show better responses to the slippage occurrence due to the mechanism of adhesion friction (Carbone *et.al.*, 2009). But when the contacting occurs between the fingertips soft layers and the pair of wood layers of the grasped object, the experimental results of this case of contact show noise and unclear responses. This is due to the variety in the mechanism of friction of soft with wood. As a summary, the present approach can detect the onset of slip of the grasped object with different roughness i.e. smooth layer (glass) and rough layer (wood).

Figures (21 and (23) is divided into five subfigures, each subfigure display the normalized ratios components of contact forces with specific slippage angle ( $0^\circ$  or  $45^\circ$  or  $90^\circ$ ) and with a specific contact material (glass or wood). By monitoring the behavior of the normalized ratios of components of contact forces, one can notice that the overall signals of the normalized ratios have the same behavior almost at the slippage occurrence period which is interpreted as a jumping off from the initial value of the ratio. It also

notes that there exists a slight diversity in the onset of slippage at each contact force ratio ( $F_t/F_n(1R)$ ,  $F_t/F_n(2R)$ ,  $F_t/F_n(1L)$ ,  $F_t/F_n(2L)$ ). This is due to the mismatch of the grasp area in both fingers on the two sides of the grasped object; moreover, it is not ensured that the external load which is applied to generate the slip will be in the tangential direction of the angle of the slippage occurrence. This diversity can be considered as a special feature added to the features of the controlling system because the controller can detect the slip at any time and direction.

**5.3.2 Second group of experiments:** Control the slippage under dynamic load cases.

As mentioned in subsection (5.1.2), the grasped object in this group is under the effect of localized disturbance (dynamic load). This load is generated by means of two disturbance generators (unbalance DC motors) embedded within the grasped object. In these experiments, the object will be grasped just under its weight until it reaches the stable status of grasp. Then, the overall signals of the sensory system will be recorded, afterwards turning-on the two unbalance DC motor simultaneously to generate an excitation in the grasped object till the object begins to slip. Finally, recording the response of neural network, which operates on stopping the slippage by increasing the grasping force, the results of this group will be listed as follows:

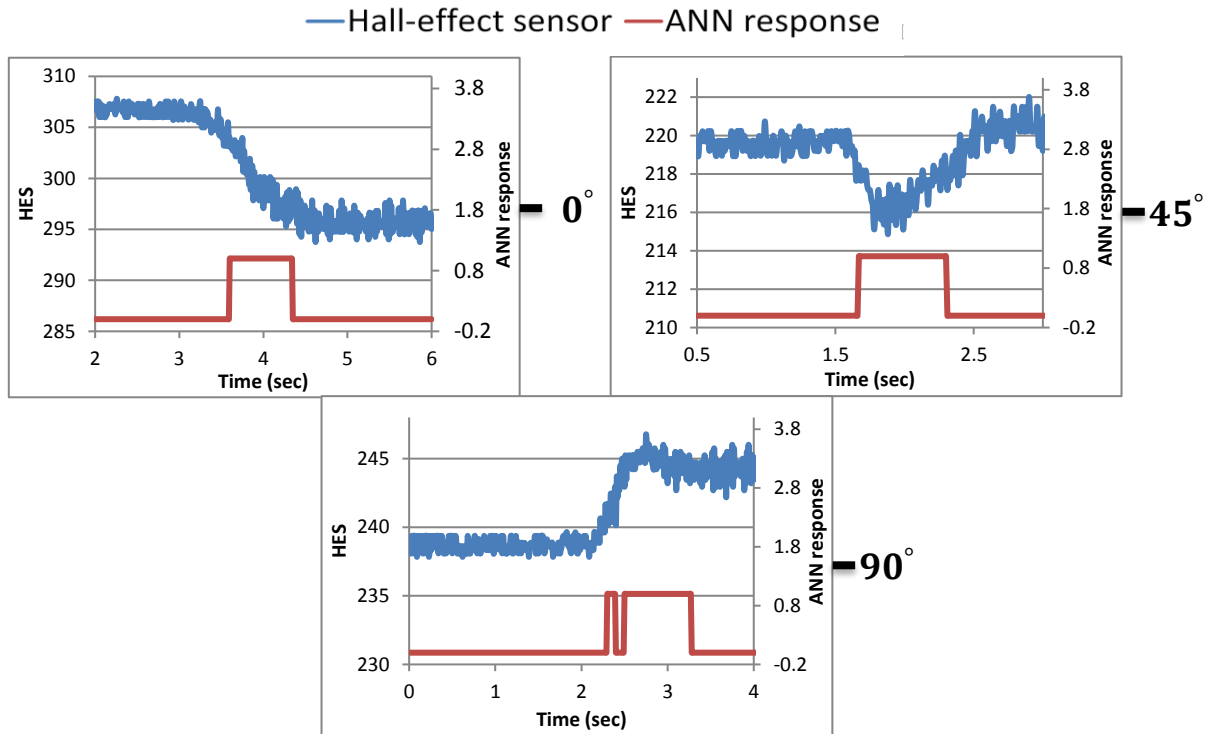


**Figure (24):** The system control response under dynamic load and different slippage angles, glass layer.

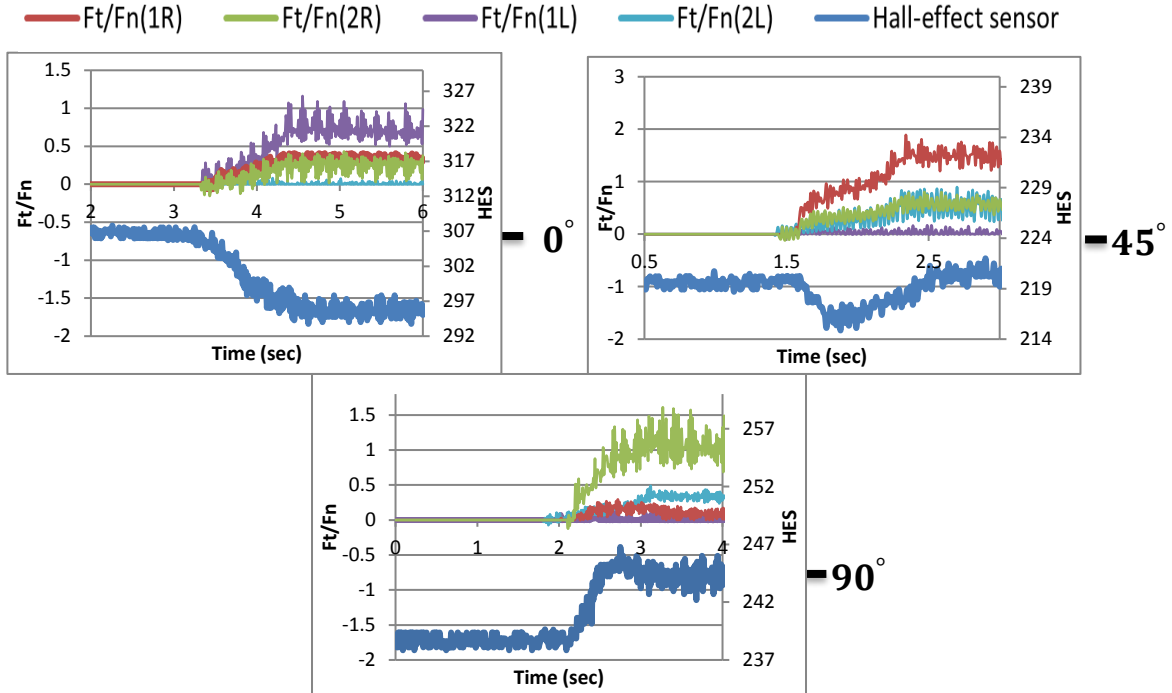


Figure (25): The normalized force ratios under dynamic load and different slippage angles, glass layer.

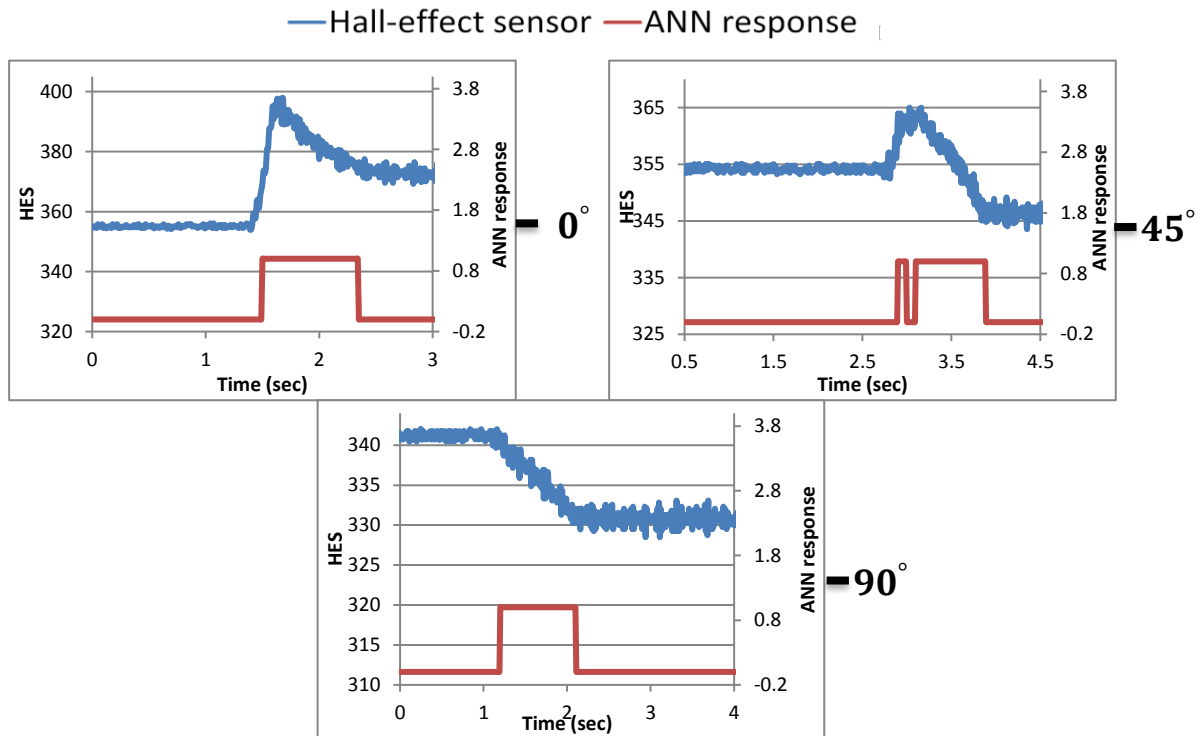
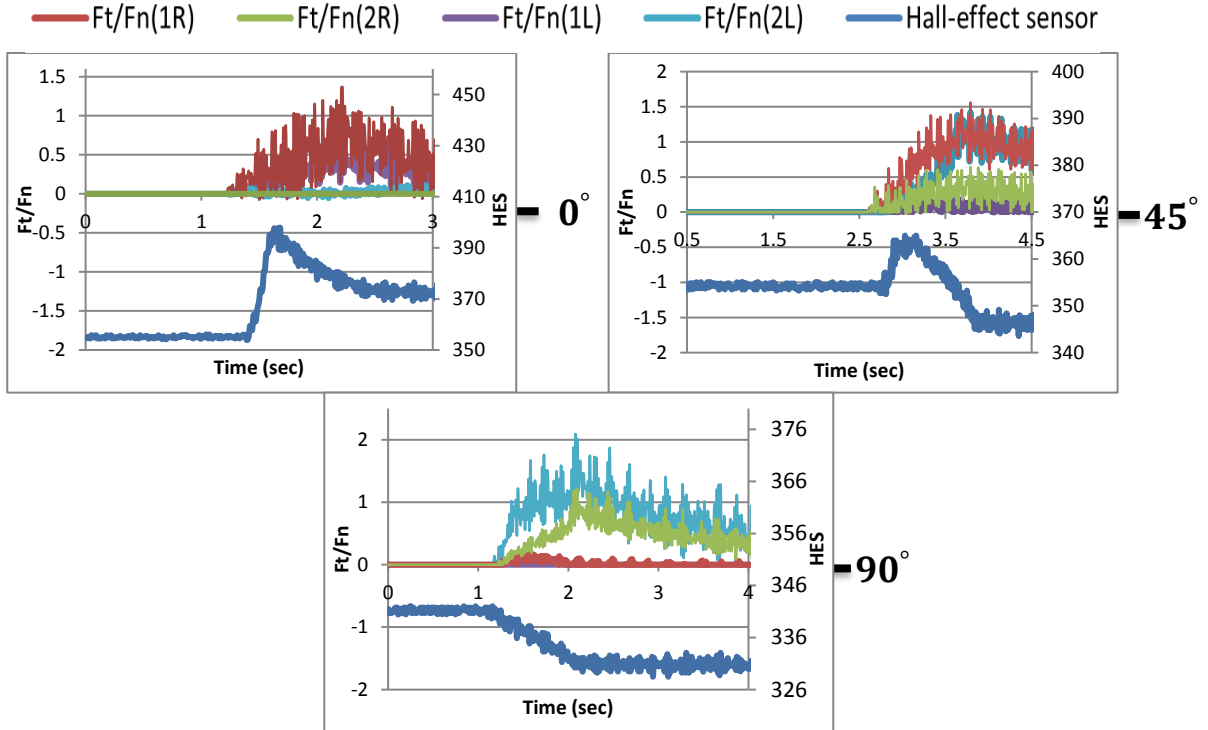


Figure (26): The system control response under dynamic load and different slippage angles, wood layer.



**Figure (27): The normalized force ratios under dynamic load and different slippage angles, wood layer.**

Figures (24) and (26) show the response of the controlling system under dynamic load effect in comparison with the hall-effect sensor signal. The artificial neural network in this group of experiments has been tested. It is capable of distinguishing the slippage and gives its response at this moment, where these experiments are conducted with multi-direction slip occurrence and with two types of contact material (glass and wood). The control system has demonstrated similar behavior to that of the first group of experiments, i.e. the neural network can give a response to the occurrence of slippage regardless of the type of the load that causes the slippage.

Each subfigure in figures (25) and (27) clarifies the signals of normalized ratios of contact force components with a certain direction to slip and with a certain contact material. The control system showed its ability to give a good response to the variety in the signals of the normalized ratios which happened because of the effect of slipping. In other words, the experimental results of this group revealed that the control system able to distinguish between the variation of the normalized ratios caused by the effect of the dynamic load and the variation caused by the effect of slipping. The experiments also showed that there was diversity between each normalized ratio and other. This happened as a result of the moment of slippage occurrence, the diversity in the situation of the grasping, the non-asymmetry in the two unbalance DC motor operating and the difference in the friction coefficient for each contact material (glass and wood) which leads to different behavior of the signal of the normalized ratios. Eventually, the flexible parts (compressive springs) in the fingertip mechanism may affect the overall type of tests

(first and second groups of experiments). This has been caused the diversity in the normal component and the two tangential components.

## 6. Conclusion

The artificial gripper has been controlled in order to provide a stable grasp situation. In other words, making and optimization process of grasping forces by the detection of slip between the grasped object and artificial fingers. Whether the grasping forces are slight, this leads to slip and whether the grasping forces are high, this leads to a breakdown of the grasped object. For this purpose, the ANN has been exploited by training on the detection of the slip by distinguishing the pattern of the slippage signals which are represented by the contact force components ratio signals ( $F_{t_i}/F_{n_i}$ ). This operation has been done by helping of Matlab/Simulink program. The problems that associate with the noise of the FlexiForce sensors and the pairing of contact material (glass and wood) of the object have been eliminated by means of the normalization process. For the future work, the present study has to be developed by enhancing the performance of the neural network algorithm to be able to train online i.e. the weights and bias functions will be updated when the grasping being in real environment.

## 7. Nomenclature

$F_{s_i}^L, F_{s_i}^R$  Forces measured by Flexiforce sensors for left and right finger respectively

$f_i^L, f_i^R$  Springs forces at fingertips for left and right finger respectively

$F_n^L, F_n^R$  Normal components of contact forces for left and right finger respectively

$F_{t_i}^L, F_{t_i}^R$  Tangential components of contact forces for left and right finger respectively

$F_{t_i}/F_{n_i}$  Ratio of tangential force to normal force

$\mu_s$  Static coefficient of friction

$\mu_d$  Dynamic coefficient of friction

## 8. References

- Abdulrahman Abdulkareem S. Al-Shanoon, Siti Anom Ahmad and Mohd. Khair B. Hassan, 2016, "Re-gripping analysis based on implementation of slip-detection device for robotic hand model", Region 10 Symposium (TENSYP) IEEE.
- Ikeda A., Kurita Y., Ueda J., Matsumoto Y., Ogasawara T., 2004, "Grip Force Control for an Elastic Finger using Vision-based Incipient Slip Feedback", In Proceedings of IEEE International Conference on Intelligent Robots and Systems September 28 - October 2, Sendai, Japan.
- Mazid A. and Fakhrul Islam M. , 2008, "Grasping force estimation recognizing object slippage by tactile data using neural network", in Proceeding of IEEE Conference of Robotic, Automation and Mechatronics, 21–24 September.

Schürmann C., Schöpfer M. and Haschke R. , 2012, "A High-Speed Tactile Sensor for Slip Detection", Springer Tracts in Advanced Robotics, pp 403-415, January.

“FlexiForce® Standard Model A301” online available (<https://www.tekscan.com/products-solutions/force-sensors/a301>).

Kobayashi F. , Kanno H., Nakamoto H., and Kojima F. , 2014, “Slip based pick-and-place by universal robot hand with force/torque sensors,” in IEEE Symposium on Robotic Intelligence in Informationally Structured Space, pp. 1-4, 9-12 Dec.

Carbone G. , Lorenz B. , Persson B. N. J. and Wohlers A. , July, 2009," Contact mechanics and rubber friction for randomly rough surfaces with anisotropic statistical properties", The European Physical Journal E, Vol. 29, Issue 3, pp 275–284.

“Hall-Effect Sensor 49E”, online available (<https://chioszrobots.com/2015/03/26/hall-magnetic-standard-linear-module-arduino-projects-robots-new/>).

Fusjimoto I., Yamada Y., Maeno T. , Aug. 2003, “Development of Artificial Finger Skin to Detect Incipient Slip for Realization of Static Friction Sensation”, In Proceedings of IEEE International Conference on Multisensor Fusion and Integration for Intelligent Systems MFI, pp.15-21.

Joonhee Jo, Sung-kyun Kim, Yonghwan Oh, and Sang-Rok Oh, 20–24 August 2012, "Contact force control of a robotic hand using F/T sensory feedback with a rigid object", In: IEEE international conference on automation science and engineering, Seoul, Korea, , pp.436–441. New York.

Mark R. Cutkosky, June 1989 , "On Grasp Choice, Grasp Models, and the Design of Hands for Manufacturing Tasks", IEEE Transaction on Robotics and Automation, Vol.5, No.3, pp.269-279.

" Multilayer Neural Network Architecture", online available (<https://www.mathworks.com/help/nnet/ug/multilayer-neural-network-architecture.html>).

Elango N. and Faudzi A. A. M. , September, 2015 , " A review article: investigations on soft materials for soft robot manipulations", The International Journal of Advanced Manufacturing Technology, Vol. 80, Issue 5–8, pp 1027–1037.

Peng Chen, Yoshizo Hasegawa and Mitushi Yamashita, May, 2006, “Grasping control of robot hand using fuzzy neural network”, In International Symposium on Neural Networks (pp. 1178-1187). Springer Berlin Heidelberg.

Raul Fernandez, Ismael Payo, Andres S. Vazquez and Jonathan Becedas, 3 January 2014, “Micro-Vibration-Based Slip Detection in Tactile Force Sensors”, Sensors 2014, 14(1), 709-730.

Herrera R., 6–8 April, 2011, "Bio-inspired tactile control for dexterous manipulation of unknown objects", in International Workshop on Bio-Inspired Robots.

Shouhei Shirafuji and Koh Hosoda, January, 2014, "Detection and prevention of slip using sensors with different properties embedded in elastic artificial skin on the basis of previous experience", *Journal of Robotics and Autonomous Systems*, Vol. 62, Issue 1, Pages 46-52.

Somer M. Nancy, Mauwafak A. Tawfik and Ihsan A. Baqer, 2016, "A Novel Approach to Control the Robotic Hand Grasping Process by Using an Artificial Neural Network Algorithm", *Journal of Intelligent System*, Vol.26, Issue 2.

Su, Z., Hausman, K., Chebotar, Y., Molchanov, A., Loeb, G. E., Sukhatme, G. S., & Schaal, S. ; Jul 2015, "Force Estimation and Slip Detection for Grip Control using a Biomimetic Tactile Sensor" proceedings of the IEEE-ARS. International Conference on Humanoid Robotics (Humanoids).